ARTICLE
PUBLISHED ONLINE: 16 MARCH 2014 | DOI: 10.1038/NCHEMBIO.1479
nature chemical biology

G-quadruplexes regulate Epstein-Barr virus–encoded nuclear antigen 1 mRNA translation

Pierre Murat[1], Jie Zhong[2,3], Lea Lekieffre[2,3], Nathan P Cowieson[4], Jennifer L Clancy[5], Thomas Preiss[5], Shankar Balasubramanian[1,6,7], Rajiv Khanna[2,3] & Judy Tellam[2,3]*

Viruses that establish latent infections have evolved unique mechanisms to avoid host immune recognition. Maintenance proteins of these viruses regulate their synthesis to levels sufficient for maintaining persistent infection but below threshold levels for host immune detection. The mechanisms governing this finely tuned regulation of viral latency are unknown. Here we show that mRNAs encoding gammaherpesviral maintenance proteins contain within their open reading frames clusters of unusual structural elements, G-quadruplexes, which are responsible for the *cis*-acting regulation of viral mRNA translation. By studying the Epstein-Barr virus–encoded nuclear antigen 1 (EBNA1) mRNA, we demonstrate that destabilization of G-quadruplexes using antisense oligonucleotides increases EBNA1 mRNA translation. In contrast, pretreatment with a G-quadruplex–stabilizing small molecule, pyridostatin, decreases EBNA1 synthesis, highlighting the importance of G-quadruplexes within virally encoded transcripts as unique regulatory signals for translational control and immune evasion. Furthermore, these findings suggest alternative therapeutic strategies focused on targeting RNA structure within viral ORFs.

Translational control of protein synthesis is a fundamental process universal to all eukaryotes and prokaryotes and is crucial for diverse biological processes including metabolic homeostasis, cellular differentiation, proliferation and transformation. The multistep pathway of protein synthesis can be regulated at the level of translation initiation, elongation and termination[1]. Many pathogens infecting humans exploit these regulatory translational steps to replicate and disseminate in the wider population. Of particular interest are members of the viral family Herpesviridae, which have co-evolved with *Homo sapiens* over millions of years and are associated with a range of malignancies[2]. Following infection, gammaherpesviruses such as Epstein-Barr virus (EBV) and Kaposi sarcoma herpesvirus use various strategies to downregulate viral protein synthesis and thereby restrict antigen presentation to cytotoxic T cells through the MHC class I pathway[3]. These immune evasive strategies are implicated in the pathogenesis of EBV-associated malignancies such as Burkitt's lymphoma, nasopharyngeal carcinoma and Hodgkin's lymphoma[4].

The latency program of gammaherpesviruses is critically reliant on a unique class of viral proteins referred to as genome maintenance proteins, which have been shown to inhibit their self-synthesis by an undefined mechanism[3]. An overrepresentation of purine codons within the coding sequence of the Epstein-Barr virus maintenance protein, EBNA1 (ref. 5), correlates with an inhibition of mRNA translation and restricted endogenous presentation of $CD8^+$ T-cell epitopes[6]. This purine bias is specifically observed within the region encoding the EBNA1 internal glycine-alanine repeat domain (GAr), which is critical for regulating EBNA1 self-synthesis and thereby for minimizing immune recognition[7–20]. Reduction of purine codons within the EBNA1 GAr domain through codon modification markedly reverses this inhibitory effect[6]. Moreover, diverse EBNA1 GAr peptide sequences resulting from alternative reading frames do not alleviate the inhibitory effect on both EBNA1 self-synthesis and the presentation of EBNA1 epitopes[17] and suggest that regulatory structural elements within the EBNA1 GAr encoding mRNA itself might regulate mRNA translation and antigen presentation.

In this study we have used a combination of biophysical and immunological techniques and demonstrated how unique clusters of unusual RNA secondary structures, G-quadruplexes, within the EBNA1 GAr encoding mRNA act as critical *cis*-regulatory elements of mRNA translation. We also revealed that G-quadruplexes are similarly observed in other gammaherpesviral maintenance gene mRNAs that are known to regulate their self-synthesis. Furthermore, our findings demonstrated that altering the stability of EBNA1 G-quadruplexes using either antisense oligonucleotides or small-molecule G-quadruplex–binding ligands had a strong impact on mRNA translation and antigen presentation.

RESULTS

EBNA1 mRNA sequence contains G-quadruplex clusters

Because of an extreme overrepresentation of guanines (62%) within the EBNA1 GAr mRNA, we explored the possibility that this purine-rich repetitive sequence may form RNA G-quadruplex structures. G-quadruplexes are secondary structures of nucleic acids that form within G-rich DNA or RNA sequences. These structures are stabilized by the stacking of guanine tetrads, which are formed by the coplanar arrangement of four G bases interacting by Hoogsteen hydrogen bonding (**Fig. 1a**,**b**)[21]. G-quadruplexes, which are increasingly implicated in diverse biological processes including replication, transcription and translation[22–24], are present in telomeres, promoters and gene bodies, where they perform important regulatory roles[22,25,26].

An analysis of the EBNA1 GAr mRNA revealed G nucleotides organized into repeats of characteristic putative G-quadruplex

[1]Department of Chemistry, University of Cambridge, Cambridge, UK. [2]Tumour Immunology, Department of Immunology, Clive Berghofer Cancer Research Centre, QIMR Berghofer Medical Research Institute, Brisbane, Queensland, Australia. [3]QIMR Centre for Immunotherapy and Vaccine Development, QIMR Berghofer Medical Research Institute, Brisbane, Queensland, Australia. [4]Centre for Synchrotron Science, Monash University, Melbourne, Victoria, Australia. [5]Genome Biology Department, The John Curtin School of Medical Research, The Australian National University, Canberra, Australian Capital Territory, Australia. [6]Cambridge Institute, Cancer Research UK, Li Ka Shing Center, Cambridge, UK. [7]School of Clinical Medicine, The University of Cambridge, Addenbrooke's Hospital, Hills Road, Cambridge, UK. *e-mail: judy.tellam@qimr.edu.au

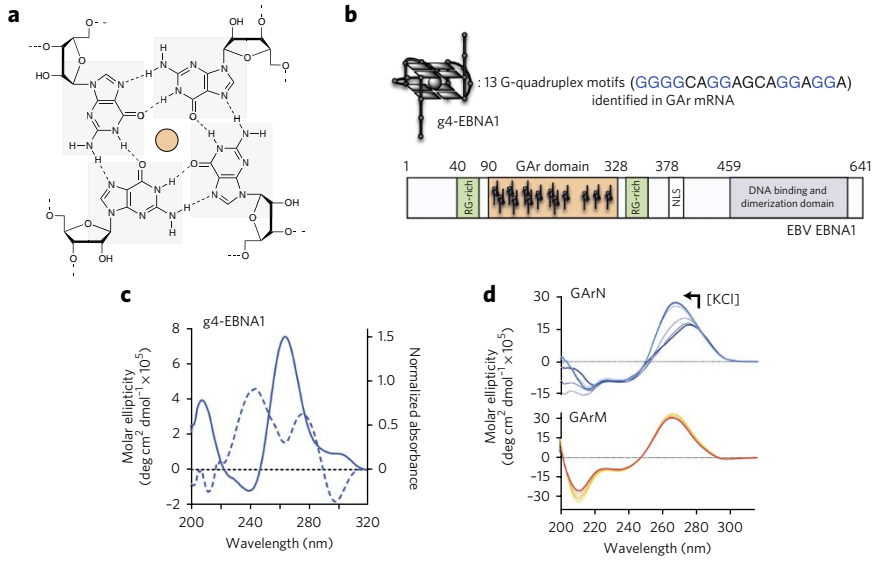

Figure 1 | Identification and characterization of G-quadruplex structure within the EBNA1 GAr mRNA. (**a**) A guanine tetrad formed by the coplanar arrangement of four guanine bases held together by Hoogsteen hydrogen bonds and stabilized by a cation (usually potassium, depicted in orange). (**b**) Schematic representation of EBV EBNA1 depicting the domains essential for genome maintenance functions[3]. Highlighted within the internal GAr domain are the positions of g4-EBNA1 G-quadruplex motifs identified in the corresponding mRNA. The g4-EBNA1 schematic depicts an EBNA1 intramolecular parallel G-quadruplex stabilized by the stacking of two guanine tetrads (gray squares represent guanines as depicted in **a**). (**c**) Characterization of the g4-EBNA1 G-quadruplex by CD and UV spectroscopy. The CD (unbroken line) and normalized thermal difference (dashed line) spectra of g4-EBNA1 in the presence of K^+. (**d**) CD titration spectra of a 300-nucleotide native EBNA1 GAr transcript (GArN) and a 300-nucleotide codon-modified EBNA1 GAr transcript (GArM) with increasing KCl concentration (0–100 mM).

sequence (PQS) of the form ($G_{2+}N_{1-7}G_{2+}N_{1-7}G_{2+}N_{1-7}G_{2+}$), where N is any base, including G. The EBNA1 mRNA contained clusters of PQS motifs extending over 74% of the repeat sequence (**Fig. 1b** and **Supplementary Results**, **Supplementary Table 1** and **Supplementary Note**). To determine the relevance of the multiple G-quadruplex motifs identified within the EBNA1 GAr mRNA sequence, we examined an 18-nucleotide G-rich sequence (GGGGCAGGAGCAGGAGGA; referred to as g4-EBNA1 and coding for Gly-Ala-Gly-Ala-Gly-Gly) occurring 13 times throughout the repeat sequence (**Fig. 1b** and **Supplementary Note**) and assessed its ability to form a G-quadruplex *in vitro*.

CD spectroscopy and UV thermal difference spectra both confirmed the ability of g4-EBNA1 to fold into a parallel G-quadruplex structure, as characterized by a maximum ellipticity at 266 nm and a minimum at 240 nm in the CD spectrum and by a negative minimum at 295 nm in the thermal difference spectra (**Fig. 1c** and **Supplementary Fig. 1**)[27,28]. UV-thermal denaturation studies at 295 nm demonstrated a hypochromic potassium-dependent transition that was independent of the oligodeoxynucleotide concentration, which is consistent with intramolecular G-quadruplex formation. In addition, we observed some hysteresis for UV melting-cooling curves, which demonstrated slow folding kinetics of g4-EBNA1 G-quadruplex motifs (**Supplementary Fig. 1**). The ^{1}H NMR spectrum of g4-EBNA1 demonstrated broad imino peaks in the range of 10.5–11.5 p.p.m. characteristic of the formation of guanine tetrads involved in inhomogeneous G-quadruplex structures (**Supplementary Fig. 2**)[29] and further supported the view that g4-EBNA1 was able to fold into an intramolecular parallel G-quadruplex *in vitro* with a thermal stability of 54.1 ± 1.1 °C (mean ± s.d., $n = 3$) in a potassium ion–dependent manner.

We next assessed the potential of g4-EBNA1 to form stable G-quadruplex structures within the mRNA repeat. CD spectroscopy was used to study the influence of K^+ on a native EBNA1 GAr transcript (referred to as GArN) (**Supplementary Figs. 3** and **4**). In the absence of K^+, the CD spectrum exhibited a maximum ellipticity at 275 nm (**Fig. 1d**). Upon addition of K^+, the maximum was displaced to 266 nm (**Fig. 1d**), and the molar ellipticity increased (**Supplementary Fig. 5**), reflecting a potassium-dependent folding of the GArN transcript. As G-quadruplex formation is dependent on the presence of potassium and parallel G-quadruplexes are characterized by a maximum at 266 nm[27], these results demonstrated that G-quadruplexes form within EBNA1 mRNA. In contrast, a corresponding codon-modified EBNA1 GAr transcript (referred to as GArM), designed to reduce purine bias while maintaining the encoded native protein sequence[6] and in so doing initiate stem-loop structure, did not show a similar potassium dependency (**Supplementary Fig. 5**), and its CD spectrum was characterized by a minimum at 210 nm (**Fig. 1d** and **Supplementary Figs. 3** and **4**). This latter spectral signature was attributed to the A-form of the double helix[27], i.e., RNA duplexes, and confirmed stem-loop structures as the major component of a codon-modified EBNA1 GAr mRNA. These results demonstrated that potassium-dependent G-quadruplexes are the major structural components of the native purine-rich EBNA1 GAr mRNA, whereas RNA duplexes are the major component of a codon-modified EBNA1 GAr mRNA owing to altered base pairing following purine reduction. Further analysis of the native and codon-modified EBNA1 transcripts using small-angle X-ray scattering (SAXS) to measure the mean square radius of the cross section (R^2_{cs}) of each mRNA supported the CD spectral results and demonstrated a more compact native EBNA1 GAr mRNA (with a cross-section radius estimated to be less than 20 Å) compared to an identically matched codon-modified EBNA1 GAr mRNA (with a cross section radius of 86.5 Å; **Supplementary Fig. 6a**). These observations were also consistent with MFold predictions of the codon-modified GAr mRNA folding into double-stranded structures, whereas the native EBNA1 GAr mRNA lacked a similar stem-loop structure (**Supplementary Fig. 6b**)[6]. Notably, the bulges predicted for the native GAr mRNA by MFold analysis, which does not take into account G-quadruplex structure, encompass G-rich sequences such as g4-EBNA1, i.e., G-quadruplex motifs. In summary, we have identified an unusual secondary structure that forms into clusters within the EBNA1 GAr mRNA (74% of the EBNA1 GAr mRNA is covered by PQS; **Supplementary Note**), possibly reflecting an allosteric regulation of the folding of the G-rich repeat.

Having demonstrated G-quadruplex structures within the EBNA1 GAr mRNA, we hypothesized that similar PQS motifs also existed within the conserved purine-rich sequences of other gammaherpesviral genome maintenance proteins (GMPs). Indeed, our initial computational analysis of eight purine-rich mRNAs encoding gammaherpesviral GMPs revealed the presence of multiple PQS motifs (**Supplementary Table 1**). The GMP mRNAs, half of which have been implicated in immune evasion, contained clusters of PQS motifs extending over 10–81% of their respective purine-rich repeat sequences (**Supplementary Table 1** and **Supplementary Note**)[3,6]. The PQS sequences from the eight GMP viral ORF repeats were analyzed by CD and ^{1}H NMR spectroscopy, and all of them

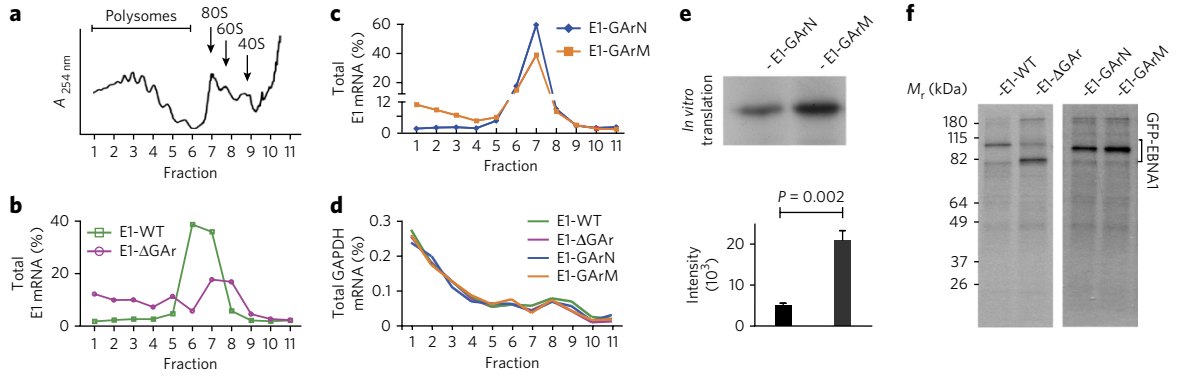

Figure 2 | Codon modification enhances EBNA1 mRNA translation by destabilizing G-quadruplex structures. (**a**) Representative polysome gradient profile absorbance trace at 254 nm shows the position of polysomes, ribosomes, (80S) and subunits (60S, 40S). (**b**) Polysome distribution profiles comparing the translation of E1-WT and E1-ΔGAr. (**c**) Polysome distribution profiles comparing the translation of EBNA1 transfectants expressing 500 nucleotides of native GAr mRNA, E1-GArN and the codon-modified GAr mRNA E1-GArM. (**d**) Polysome profile of the endogenous GAPDH mRNA observed by RT-qPCR for each EBNA1 variant. (**e**) IVT assay of EBNA1 expression constructs expressing 300 nucleotides of native GAr mRNA, E1-GArN or the codon-modified GAr mRNA E1-GArM (**Supplementary Fig. 8**). Band intensities were quantified by densitometric analysis (data represent mean values ± s.e.m.; $n = 3$). (**f**) Autoradiograph showing the relative mRNA translation efficiencies of GFP-E1-WT, GFP-E1-ΔGAr and GFP-EBNA1 encoding 500 nucleotides of native GAr mRNA, GFP-E1-GArN or the codon-modified GAr mRNA GFP-E1-GArM. HEK293 cells transfected with GFP-EBNA1 vectors were pulsed with [^{35}S]methionine, and lysates were immunoprecipitated with antibodies to GFP and subjected to SDS-PAGE and autoradiography. M_r, molecular weight markers.

had spectral signatures consistent with parallel G-quadruplex formation[27,29] (**Supplementary Fig. 7**), suggesting that gammaherpesviruses exploit RNA G-quadruplexes as structural regulatory elements.

EBNA1 G-quadruplexes modulate mRNA translation

To investigate the impact of G-quadruplex structures on EBNA1 translation, we analyzed polysome distribution profiles (**Fig. 2a–d**)[30] of EBNA1 transfectants expressing either native, codon-modified or no-GAr repeats. We speculated that G-quadruplex motifs within the GAr mRNA may inhibit elongation by inducing ribosome dissociation, as an earlier study had reported that the inhibition of EBNA1 synthesis was not due to interference of translation initiation[9]. Comparison of mRNA polysome profiles of wild-type EBNA1 (E1-WT) and EBNA1 lacking its GAr (E1-ΔGAr) revealed that the presence of the native GAr mRNA reduced ribosome occupancy (presumably owing to ribosome drop-off or premature termination), as demonstrated by an accumulation of E1-WT mRNA in subpolysomal fractions (**Fig. 2b**). In contrast, markedly greater polysome densities were associated with E1-ΔGAr mRNA (**Fig. 2b**), consistent with the observed increased translation of transcripts lacking the GAr sequence and confirming involvement of the GAr mRNA in impeding EBNA1 translation. This result solely reflects translation events as modification or deletion of the GAr sequence did not affect steady-state mRNA levels of EBNA1 (refs. 16,19) and is consistent with a mechanism in which G-quadruplex structures present a steric block to the transit of ribosomes, thereby inducing ribosome stalling and/or dissociation.

We next assessed whether native GAr mRNA G-quadruplex structures were more likely to induce ribosome dissociation compared to codon-modified GAr mRNA structures by comparing the polysome profiles of EBNA1 transfectants expressing either native GAr mRNA (E1-GArN) or codon-modified GAr mRNA (E1-GArM) (**Supplementary Fig. 4**). Data presented in **Figure 2c** demonstrate that codon modification of the GAr mRNA, to destabilize G-quadruplex structure, increased the translated pool of mRNAs (fractions 1–5) from 9% to 34%, consistent with an introduced stem-loop structure resulting in reduced ribosome dissociation. The increased translational efficiency most likely reflected the impact of secondary structures on translation elongation rather than rare codons within the GAr sequence leading to slow elongation through the GAr, as EBNA1 mRNA translation efficiency is not sensitive to frameshift mutations[17]. To confirm the validity of the observed changes in each of the EBNA1 mRNA profiles, we determined the corresponding endogenous GAPDH mRNA by RT-qPCR and observed virtually identical GAPDH profiles from each EBNA1 gradient (**Fig. 2d**). These results demonstrated that ribosomes seem to transit more efficiently through double-stranded structures compared to G-quadruplex structures, suggesting that G-quadruplexes may be less efficient at being resolved by the ribosome machinery. The reduced translational efficiency of a native EBNA1 mRNA was also confirmed by *in vitro* translation (IVT) assays where E1-GArN was less efficiently translated compared to E1-GArM (**Fig. 2e** and **Supplementary Fig. 8**). In addition, [^{35}S]methionine pulse labeling experiments were performed to determine the relative mRNA translational efficiencies of GFP-EBNA1 variants expressing either wild-type EBNA1 (GFP-E1-WT), EBNA1 with no repeat (GFP-E1-ΔGAr), EBNA1 encoding a native GAr mRNA (GFP-E1-GArN) or a codon-modified GAr mRNA (GFP-E1-GArM) (**Supplementary Fig. 4**). Results presented in **Figure 2f** demonstrate that the GFP-E1-WT mRNA was translated 45–50% less efficiently compared to the GFP-E1-ΔGAr mRNA, and, similarly, the GFP-E1-GArN mRNA was translated 50–55% less efficiently than the GFP-E1-GArM mRNA. As the GAr contains only glycine and alanine residues, the above GFP-EBNA1 variants contained equal numbers of methionine residues, and therefore these results demonstrated that the difference in GFP-EBNA1 protein products solely reflected the translational efficiency of the different GFP-EBNA1 mRNAs. These findings confirmed both the polysome profiling and IVT results and further emphasized the critical role of G-quadruplexes in regulating EBNA1 self-synthesis.

Destabilizing G-quadruplexes enhances mRNA translation

We next assessed the potential of exogenous factors to destabilize g4-EBNA1 structures and stimulate translation after having demonstrated that codon modification of the native GAr mRNA destabilized g4-EBNA1 structures and overcame their inhibitory effect on translation. A series of antisense oligonucleotides complementary to the EBNA1 GAr mRNA were tested for their ability to 'open' g4-EBNA1 structures. We hypothesized that an unfolded or

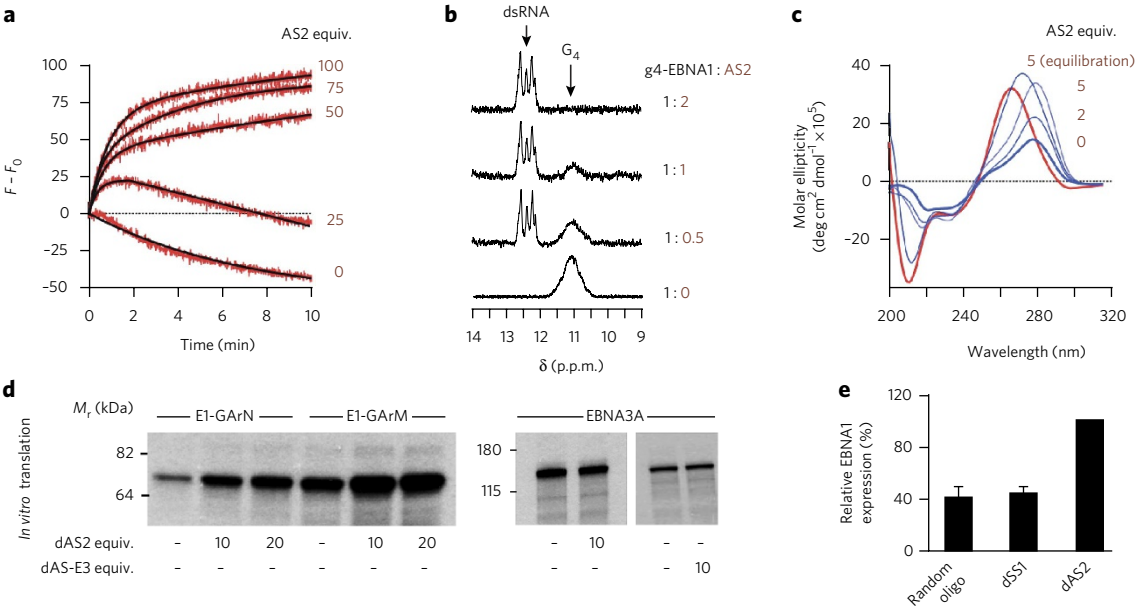

Figure 3 | The antisense oligonucleotide AS2 destabilizes g4-EBNA1 G-quadruplexes to enhance EBNA1 expression. (**a**) AS2 unfolded g4-EBNA1 in a concentration-dependent manner. Time course of the fluorescence intensity of dual-labeled g4-EBNA1 (200 nM) with increasing AS2 concentration (0.25–10 molar equiv.). g4-EBNA1 was labeled with 6-FAM and TAMRA at its 5′ and 3′ ends (excitation at 494 nm and emission at 580 nm). (**b**) Expansion of the ^{1}H NMR spectra of g4-EBNA1 when titrated with increasing AS2 concentration. Hoogsteen imino peaks disappeared during AS2 titration in favor of Watson-Crick imino peaks, characterized by a chemical shift (δ) in the range 12.0–13.0 p.p.m., demonstrating conversion of g4-EBNA1 structure to double-stranded structure. dsRNA, double-stranded RNA. (**c**) CD spectra of a 300-nucleotide native GAr transcript, GArN, in the absence (bold blue line) or presence (thin blue line) of AS2 (2 equiv., 5 equiv. and 5 equiv. after a 12-h equilibration). The CD spectrum of a 300-nucleotide codon-modified GAr transcript, GArM, is shown for comparison (red line). (**d**) IVT assays of EBNA1 constructs expressing 400 nucleotides of native GAr, E1-GArN, the codon-modified GAr E1-GArM or a G-quadruplex negative EBV-EBNA3A control construct in the presence and absence of dAS2 at increasing molar excess or an antisense deoxyoligonucleotide to EBNA3A (dAS-E3) (**Supplementary Fig. 10**). M_r, molecular weight markers. (**e**) Densitometric quantification of EBNA1 expression in EBNA1-expressing HEK293E cells following transfection with dAS2, dSS1 or a random deoxyoligonucleotide and detected by immunoblotting with antibodies to EBNA1 or β-actin. Band intensities determined the percentage of relative EBNA1 expression (data represent mean values ± s.e.m.; n = 3; **Supplementary Fig. 11a**).

destabilized g4-EBNA1 conformation would increase the translational efficiency of EBNA1. A 21-mer RNA 5′-(UCC UGC CCC UCC UCC UGC UCC)-3′ antisense oligonucleotide and its DNA analog, referred to as AS2 and dAS2, respectively, were synthesized and shown by fluorescent trap assays[31], NMR spectroscopy and gel electrophoresis to efficiently unfold g4-EBNA1 (**Fig. 3a**,**b** and **Supplementary Fig. 9**). Both AS2 and dAS2 showed a similar ability to trap the g4-EBNA1 G-quadruplex into a g4-EBNA1–dAS2 double-stranded structure in a concentration-dependent manner (**Fig. 3a** and **Supplementary Fig. 9**). The dAS2 oligonucleotide was subsequently used in all EBNA1 expression experiments, IVT assays and antigen presentation assays owing to the instability of single-stranded RNA oligonucleotides. We first assessed the effect of AS2 on the native GAr mRNA using CD spectroscopy and demonstrated that titration of the native GAr mRNA with increasing AS2 concentrations substantially altered the structure of this transcript (**Fig. 3c**). Notably, after the thermodynamic equilibrium was reached, the CD signature of the native GAr mRNA–AS2 complex was similar to the CD signature of the codon-modified GAr mRNA. This was characterized by a CD spectral minimum at 210 nm and demonstrated that following treatment with AS2, the native GAr mRNA underwent a conformational switch that favored double-stranded conformation over G-quadruplex structure. These observations were also confirmed by EBNA1 IVT assays (**Fig. 3d**). The translational efficiency of E1-GArN increased up to 3.8-fold following treatment with dAS2 in a concentration-dependent manner (**Fig. 3d** and **Supplementary Fig. 10a**,**b**). As expected, E1-GArM was less affected by dAS2 with only a 1.4-fold increase in translation efficiency (**Fig. 3d** and **Supplementary Fig. 10a**,**b**). We anticipated that any change in the EBNA1 GAr mRNA structure following treatment with dAS2 would affect translation efficiency; however, the effect was more notable following destabilization of native EBNA1 G-quadruplex motifs. This latter result demonstrated that ribosome activity resolves double-stranded, dAS2–g4-EBNA1 complexes more easily than G-quadruplex structures and confirmed the inhibitory role of G-quadruplex structures on EBNA1 translation. The specificity of the antisense oligonucleotide approach was confirmed by the inability of dAS2 to influence the translation of a control mRNA, EBV-encoded nuclear antigen 3 (EBNA3A), which does not contain G-quadruplex structures (**Fig. 3d** and **Supplementary Fig. 10c**,**d**). Further evidence that G-quadruplex destabilization increases translation was demonstrated by an EBNA3A IVT assay where a complementary 21-mer antisense deoxyoligonucleotide to EBNA3A (dAS-E3) showed no stimulatory effect on the translation of the EBNA3A mRNA (**Fig. 3d** and **Supplementary Fig. 10c**,**d**). Similarly, a control 21-mer antisense deoxyoligonucleotide (dAS-Mod) complementary to the codon-modified GAr of E1-GArM did not stimulate E1-GArN or E1-GArM mRNA translation, unlike the stimulatory effect we observed from dAS2 targeting the corresponding region of GArN (**Supplementary Fig. 10e**,**f**).

In the next set of experiments, we extended the G-quadruplex destabilization studies to determine the impact of using an antisense oligonucleotide on EBNA1 steady-state protein levels *in vivo*. EBNA1-expressing HEK293E cells were transfected with either dAS2, a GAr sense strand deoxyoligonucleotide (referred to as dSS1) or a random DNA deoxyoligonucleotide and then were assessed for

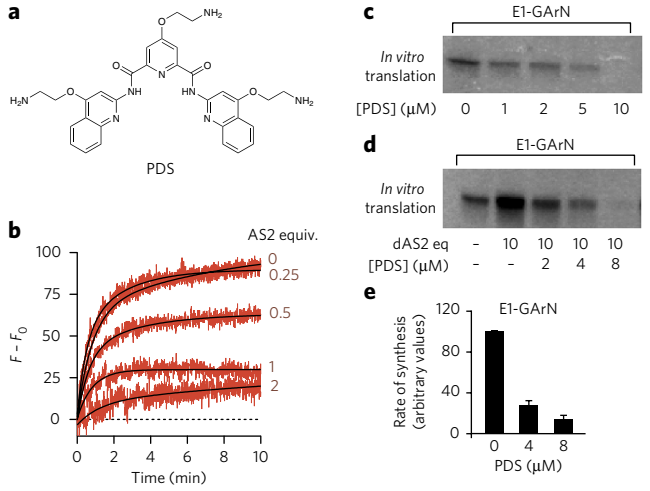

Figure 4 | The small molecule PDS stabilizes g4-EBNA1 G-quadruplex structure and inhibits EBNA1 translation. (**a**) Structure of PDS. (**b**) PDS stabilizes g4-EBNA1 in a concentration-dependent manner in the presence of AS2. Fluorescence intensity (F–F_0) time course of a dual labeled g4-EBNA1 (200 nM) in the presence of 10 molar equiv. of AS2 with increasing PDS (0 – 2 molar equiv.). The g4-EBNA1 sequence is labeled as described in **Figure 3a**. (**c**) IVT assay of an EBNA1 construct expressing 400 nucleotides of native GAr mRNA (E1-GArN) in the presence of increasing PDS concentration (**Supplementary Fig. 16a**). (**d**) IVT assay of an EBNA1 construct expressing 400 nucleotides of native GAr mRNA (E1-GArN) in the presence of an increasing molar excess of PDS and/or 10 equiv. of dAS2 (**Supplementary Fig. 17a**). (**e**) Densitometric quantification of an autoradiograph demonstrating decreased EBNA1 synthesis with increasing PDS concentration (**Supplementary Fig. 17b**). HEK293 cells transfected with a GFP-EBNA1 construct expressing 500 nucleotides of native GAr mRNA (GFP-E1-GArN) in the presence of increasing PDS concentration were pulsed with [^{35}S] methionine, and cell lysates were immunoprecipitated with antibodies to GFP, followed by SDS-PAGE. Band intensities determined the rate of EBNA1 synthesis (data represent mean values ± s.e.m.; n = 3). Molecular weight markers M_r (kDa) are indicated on the left.

EBNA1 expression. Data presented in **Figure 3e** and **Supplementary Figure 11a** demonstrate a 2.2-fold increase in EBNA1 protein expression following treatment of HEK293E cells with dAS2. Similar results were also observed when naturally infected B cells carrying an EBNA1 sequence from a B95-8 EBV bacterial artificial chromosome (BAC) were transfected with oligonucleotides dAS2 or dSS1 or a random deoxyoligonucleotide (**Supplementary Fig. 11b**). These combined data support our g4-EBNA1 *in vitro* conclusions that EBNA1 G-quadruplexes are critical regulators of EBNA1 mRNA translation.

Destabilizing G-quadruplexes enhance antigen presentation

As we had previously demonstrated that the endogenous presentation of CD8$^+$ T-cell epitopes from EBNA1 directly correlates with EBNA1 synthesis levels[16], our *in vitro* results (**Figs. 2** and **3**) suggested a modulatory role for G-quadruplexes in antigen presentation. We therefore examined the impact of dAS2 on the endogenous presentation of a MHC class I–restricted epitope fused to EBNA1. An EBNA1-GFP vector expressing native GAr mRNA and carrying a sequence encoding an H-2K^b–restricted ovalbumin epitope, SIINFEKL (E1-GArN-SIIN-GFP)[15], was transfected into HEK293KbC2 cells together with either dAS2 or a control dSS1, and transfected cells were incubated with a SIINFEKL-specific T-cell hybridoma (B3Z cells)[32]. Transfection together with dAS2 enhanced the presentation of the SIINFEKL epitope and resulted in enhanced activation of B3Z T cells at varying effector/target cell ratios compared to dSS1 (**Supplementary Fig. 12**). These observations suggest that destabilization of g4-EBNA1 in the presence of an antisense oligonucleotide not only increases the EBNA1 translational efficiency but also enhances the endogenous presentation of CD8$^+$ T-cell epitopes from the EBNA1-SIIN-GFP fusion protein.

Stabilizing EBNA1 G-quadruplexes inhibits mRNA translation

To extend our investigation of G-quadruplex regulation on EBNA1 translation, we tested a small molecule, pyridostatin (PDS; **Fig. 4a**), that is known to selectively stabilize G-quadruplex structures[33,34]. Using a fluorescence resonance energy transfer (FRET) melting assay (**Supplementary Fig. 13**)[28], we showed that PDS increased the thermal stability of g4-EBNA1 and therefore confirmed an interaction between the ligand and EBNA1 mRNA G-quadruplexes. PDS also inhibited the opening of the G-quadruplex motif by AS2 and displaced the equilibrium between the g4-EBNA1-AS2 duplex and g4-EBNA1 in favor of the G-quadruplex structure (**Fig. 4b** and **Supplementary Figs. 14** and **15**). PDS also inhibited the IVT of an EBNA1 construct expressing native GAr mRNA (E1-GArN) in a concentration-dependent manner (**Fig. 4c** and **Supplementary Fig. 16a**). The observed PDS-mediated inhibitory effect on G-quadruplex–containing mRNAs was confirmed by the lack of inhibition of an *in vitro* translated control influenza nucleoprotein mRNA lacking G-rich sequences (**Supplementary Fig. 16b**). Remarkably, IVT of E1-GArN in the presence of both dAS2 and PDS demonstrated that both exogenous agents may compete for recognition of the same G-quadruplex structural elements within the native GAr mRNA (**Fig. 4d** and **Supplementary Fig. 17a**).

Decreased EBNA1 synthesis levels observed following G-quadruplex stabilization *in vitro* was supported *in vivo* by [^{35}S] methionine pulse labeling experiments following transfection

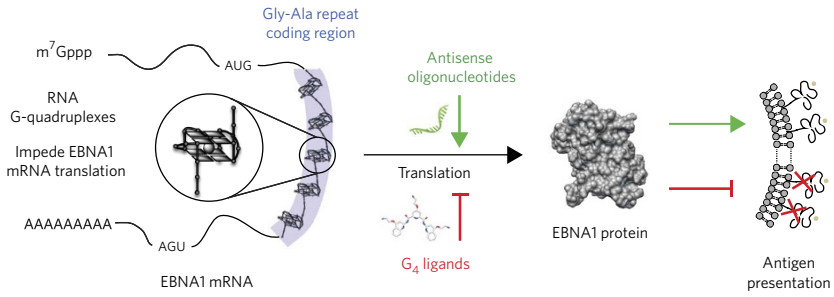

Figure 5 | A schematic summarizing the translational control of EBNA1 mRNA by *cis*-regulatory elements, G-quadruplexes, leading to immune evasion. The Epstein-Barr virus–encoded nuclear antigen 1, EBNA1, a genome maintenance protein expressed in all EBV-associated malignancies, self-regulates its synthesis levels to a degree high enough to maintain viral infection but low enough to avoid immune recognition by host virus-specific T cells. Our study demonstrated that RNA secondary structural elements, G-quadruplexes, within the EBNA1 GAr mRNA were responsible for the *cis*-acting inhibitory effect on EBNA1 synthesis, directly affecting the endogenous presentation of CD8$^+$ T-cell epitopes. Targeting the EBNA1 mRNA with an antisense oligonucleotide complementary to the g4-EBNA1 motif destabilizes the G-quadruplex structures and stimulates EBNA1 synthesis and enhances antigen presentation. Targeting the EBNA1 mRNA with a small-molecule quadruplex ligand (PDS) stabilizes the G-quadruplex structures to inhibit EBNA1 mRNA translation and decrease antigen presentation.

of HEK293 cells with a GFP-E1-GArN expression construct in the presence of increasing PDS concentrations (**Fig. 4e** and **Supplementary Fig. 17b**). The reduction in the rate of EBNA1 synthesis with increasing PDS concentrations was also confirmed following the transfection of HEK293KbC2 cells or DG75 (B cells) with E1-GArN-SIIN-GFP (**Supplementary Fig. 18a,b**). We next evaluated whether the G-quadruplex–stabilizing effect of PDS could block the endogenous presentation of CD8$^+$ T-cell epitopes from an EBNA1-SIIN-GFP fusion protein. HEK293KbC2 cells were transfected with E1-GArN-SIIN-GFP at increasing PDS concentrations and then incubated with SIINFEKL-specific B3Z T cells. As the PDS concentration was increased, the transfected cells showed a dose-dependent reduction in the activation of antigen-specific T cells, whereas the presentation of SIINFEKL-specific B3Z T-cells was unaffected in mock-treated cells (**Supplementary Fig. 18c**). These results suggest that stabilization of G-quadruplexes by PDS may further inhibit EBNA1 mRNA translation and antigen presentation, although we cannot rule out the possibility that the observed effects of PDS are in part due to its action on other mammalian genes expressed within these cells.

DISCUSSION

In this study, we have defined the mechanism by which RNA G-quadruplexes, identified within purine-rich repetitive mRNAs, slow down the translation of virally encoded maintenance proteins, thereby potentially affecting antigen presentation (**Fig. 5**). Earlier studies have reported that G-quadruplex structures perform important regulatory roles within telomeres, promoter regions and gene bodies[22,25,26], where they can influence transcription, translation and replication[22–24]. Our findings elucidate a new function of these unique structural elements where they are responsible for the *cis*-acting regulation of viral mRNA translation. We identified putative G-quadruplex sequences within the ORF of EBV-encoded EBNA1 mRNA and confirmed that these motifs form intramolecular parallel G-quadruplex structures in the context of long transcripts. Remarkably, similar G-quadruplex motifs were also mapped within the conserved purine-rich repetitive sequences of viral ORFs encoding numerous other gammaherpesviral maintenance proteins, suggesting that this class of virus may exploit RNA G-quadruplex structure to downregulate their maintenance protein expression levels to escape immune recognition. Previous RNA G-quadruplex studies hypothesized that singular stable G-quadruplex motifs present in 5′ UTR regions inhibited translation initiation[35]. In the present study, we define the role of RNA G-quadruplex motifs within purine-rich ORFs and demonstrate their ability to impede ribosomal activity during translational elongation[36]. We have shown in this study that G-quadruplex structures can alter the association of ribosomes with mRNAs by inducing premature termination and/or ribosome stalling and dissociation events. Interestingly, an earlier study demonstrated that the predominant truncated EBNA1 polypeptide prematurely terminates at approximately 19 residues into the GAr[9], which coincides with the same position where we mapped the first g4-EBNA1 motif. Furthermore, quadruplex motifs identified within the EBNA1 GAr show a moderate thermodynamic stability and high density, i.e., clusters of G-quadruplex motifs are required to ensure translational inhibition and low EBNA1 synthesis levels.

We have demonstrated that removing the G-quadruplex–containing GAr mRNA or destabilizing G-quadruplex structures through codon modification of the repetitive GAr mRNA reduces ribosome dissociation and increases EBNA1 mRNA translation. These observations are important for antigen presentation as studies from our group and others show that the translational efficiency of viral proteins directly affects the generation of rapidly degrading polypeptides (RDPs), which are the primary source of CD8$^+$ T-cell epitopes[7,9,14,15,18,37–44]. EBNA1 is an ideal model to demonstrate that CD8$^+$ T-cell epitopes are less efficiently processed from a poorly synthesized wild-type EBNA1 generating fewer RDPs compared with a more efficiently synthesized codon-modified EBNA1 where G-quadruplex structures have been destabilized, with a resultant increase in RDPs.

A similar increase in EBNA1 synthesis levels and enhanced immune recognition by antigen-specific CD8$^+$ T cells was also observed following the disruption of G-quadruplex structures in the presence of an antisense oligonucleotide complementary to the G-quadruplex sequence. Generally, small RNAs are designed to constrain expression of the target gene. The only similar mechanism to our knowledge is in the RNA activation pathway[45] and uses 21-nucleotide double-stranded RNAs to target promoter regions and activate transcription. The potential to modulate viral protein synthesis in EBV-associated and other gammaherpesvirus-associated malignancies using antisense oligonucleotides thus provides a new role for small RNA therapeutics, which goes beyond a simple on-off switch one normally associates with antisense or siRNA strategies for gene regulation. Enhancing EBNA1 mRNA translation using antisense technologies is the result of a finely balanced process as the antisense oligonucleotide is designed to invade and destabilize the G-quadruplex structures and then be displaced as the ribosome continues down the transcript. However, higher-affinity antisense analogs such as peptide nucleic acid or locked nucleic acid, while also relieving G-quadruplex repression, may then act as an obstruction to the ribosome owing to the highly stable hybrids they form, thereby blocking translation. Thus, higher-affinity oligonucleotides are likely to be undesirable from the perspective of enhancing viral mRNA translation.

In contrast to the antisense oligonucleotide stimulatory effect on EBNA1 mRNA translation, a G-quadruplex–stabilizing small molecule, PDS, decreased EBNA1 synthesis both *in vitro* and *in vivo,* resulting in EBV-infected cells being less efficiently recognized by virus-specific T cells. However, it is unclear whether the effect of the G-quadruplex ligand, PDS, solely targets EBNA1-specific G-quadruplexes *in vivo*. Notably, it is reported that protein domains within EBNA1 bind G-rich RNAs that are predicted to form G-quadruplex structures[46], suggesting a further level of regulation whereby EBNA1 protein may also self-modulate its expression using G-quadruplexes as regulatory elements. Modulation of the translational regulatory effects of these G-quadruplexes has the potential to enhance immune recognition of virally infected cells or inhibit replication of the viral genome, leading to elimination of viral latency. With no available vaccines to prevent cancers associated with EBV and other gammaherpesviruses, the identification of new therapeutic targets based on RNA G-quadruplex structures within viral maintenance mRNAs will provide new opportunities for the development of RNA-directed drug design to reduce the burden of gammaherpesvirus-associated malignancies.

By identifying a new mechanism for the control of viral mRNA translation, this study also suggested that RNA G-quadruplexes may have a more general role in the translational regulation of mammalian mRNAs as purine-rich sequences capable of potentially forming quadruplex-like structures are present in some cellular mRNAs[47]. The demonstration of clustering of G-quadruplexes in the coding regions of viral maintenance protein mRNAs and the link to regulation of protein synthesis thus suggests viral 'hijacking' of an important host cell regulatory mechanism.

Received 5 June 2013; accepted 14 February 2014;
published online 16 March 2014; corrected online 4 April 2014
(details online)

METHODS

Methods and any associated references are available in the online version of the paper.

References

1. Mathews, M.B., Sonnenberg, N. & Hershey, J.W.B. *Origins and Principles of Translational Control* (Cold Spring Harbor Laboratory Press, Cold Spring Harbor, New York, 2007).
2. Everly, D., Sharma-Walia, N., Sadagopan, S. & Chandran, B. in *Current Cancer Research* (ed. Robertson, E.S.) 133–167 (Springer, 2012).
3. Blake, N. Immune evasion by gammaherpesvirus genome maintenance proteins. *J. Gen. Virol.* **91**, 829–846 (2010).
4. Rickinson, A.B. & Kieff, E. in *Fields Virology* 3rd edn. (eds. Fields, B.N., Knipe, D.M. & Howley, P.M.) 2397–2446 (Lippincott, Williams and Wilkins, Philadelphia, 1996).
5. Cristillo, A.D., Mortimer, J.R., Barrette, I.H., Lillicrap, T.P. & Forsdyke, D.R. Double-stranded RNA as a not-self alarm signal: to evade, most viruses purine-load their RNAs, but some (HTLV-1, Epstein-Barr) pyrimidine-load. *J. Theor. Biol.* **208**, 475–491 (2001).
6. Ressing, M.E. *et al.* Epstein-Barr virus evasion of CD8$^+$ and CD4$^+$ T cell immunity via concerted actions of multiple gene products. *Semin. Cancer Biol.* **18**, 397–408 (2008).
7. Apcher, S., Daskalogianni, C., Manoury, B. & Fahraeus, R. Epstein Barr virus–encoded EBNA1 interference with MHC class I antigen presentation reveals a close correlation between mRNA translation initiation and antigen presentation. *PLoS Pathog.* **6**, e1001151 (2010).
8. Blake, N. *et al.* Human CD8$^+$ T cell responses to EBV EBNA1: HLA class I presentation of the (Gly-Ala)–containing protein requires exogenous processing. *Immunity* **7**, 791–802 (1997).
9. Cardinaud, S., Starck, S.R., Chandra, P. & Shastri, N. The synthesis of truncated polypeptides for immune surveillance and viral evasion. *PLoS ONE* **5**, e8692 (2010).
10. Lee, S.P. *et al.* CD8 T cell recognition of endogenously expressed Epstein-Barr virus nuclear antigen 1. *J. Exp. Med.* **199**, 1409–1420 (2004).
11. Levitskaya, J. *et al.* Inhibition of antigen processing by the internal repeat region of the Epstein-Barr virus nuclear antigen-1. *Nature* **375**, 685–688 (1995).
12. Mukherjee, S., Trivedi, P., Dorfman, D.M., Klein, G. & Townsend, A. Murine cytotoxic T lymphocytes recognize an epitope in an EBNA-1 fragment, but fail to lyse EBNA-1–expressing mouse cells. *J. Exp. Med.* **187**, 445–450 (1998).
13. Ossevoort, M. *et al.* The nested open reading frame in the Epstein-Barr virus nuclear antigen-1 mRNA encodes a protein capable of inhibiting antigen presentation in cis. *Mol. Immunol.* **44**, 3588–3596 (2007).
14. Tellam, J. *et al.* Endogenous presentation of CD8$^+$ T cell epitopes from Epstein-Barr virus–encoded nuclear antigen 1. *J. Exp. Med.* **199**, 1421–1431 (2004).
15. Tellam, J. *et al.* Influence of translation efficiency of homologous viral proteins on the endogenous presentation of CD8$^+$ T cell epitopes. *J. Exp. Med.* **204**, 525–532 (2007).
16. Tellam, J. *et al.* Regulation of protein translation through mRNA structure influences MHC class I loading and T cell recognition. *Proc. Natl. Acad. Sci. USA* **105**, 9319–9324 (2008).
17. Tellam, J.T., Lekieffre, L., Zhong, J., Lynn, D.J. & Khanna, R. Messenger RNA sequence rather than protein sequence determines the level of self-synthesis and antigen presentation of the EBV-encoded antigen, EBNA1. *PLoS Pathog.* **8**, e1003112 (2012).
18. Voo, K.S. *et al.* Evidence for the presentation of major histocompatibility complex class I–restricted Epstein-Barr virus nuclear antigen 1 peptides to CD8$^+$ T lymphocytes. *J. Exp. Med.* **199**, 459–470 (2004).
19. Yin, Y., Manoury, B. & Fahraeus, R. Self-inhibition of synthesis and antigen presentation by Epstein-Barr virus–encoded EBNA1. *Science* **301**, 1371–1374 (2003).
20. Zaldumbide, A., Ossevoort, M., Wiertz, E.J. & Hoeben, R.C. In *cis* inhibition of antigen processing by the latency-associated nuclear antigen I of Kaposi sarcoma herpes virus. *Mol. Immunol.* **44**, 1352–1360 (2007).
21. Parkinson, G.N., Lee, M.P. & Neidle, S. Crystal structure of parallel quadruplexes from human telomeric DNA. *Nature* **417**, 876–880 (2002).
22. Balasubramanian, S., Hurley, L.H. & Neidle, S. Targeting G-quadruplexes in gene promoters: a novel anticancer strategy? *Nat. Rev. Drug Discov.* **10**, 261–275 (2011).
23. Kumari, S., Bugaut, A., Huppert, J.L. & Balasubramanian, S. An RNA G-quadruplex in the 5′ UTR of the NRAS proto-oncogene modulates translation. *Nat. Chem. Biol.* **3**, 218–221 (2007).
24. Zhao, J., Bacolla, A., Wang, G. & Vasquez, K.M. Non-B DNA structure-induced genetic instability and evolution. *Cell. Mol. Life Sci.* **67**, 43–62 (2010).
25. Neidle, S. & Parkinson, G. Telomere maintenance as a target for anticancer drug discovery. *Nat. Rev. Drug Discov.* **1**, 383–393 (2002).
26. Rodriguez, R. *et al.* Small-molecule–induced DNA damage identifies alternative DNA structures in human genes. *Nat. Chem. Biol.* **8**, 301–310 (2012).
27. Kypr, J., Kejnovska, I., Renciuk, D. & Vorlickova, M. Circular dichroism and conformational polymorphism of DNA. *Nucleic Acids Res.* **37**, 1713–1725 (2009).
28. Mergny, J.L. *et al.* Telomerase inhibitors based on quadruplex ligands selected by a fluorescence assay. *Proc. Natl. Acad. Sci. USA* **98**, 3062–3067 (2001).
29. Phan, A.T., Kuryavyi, V., Gaw, H.Y. & Patel, D.J. Small-molecule interaction with a five-guanine-tract G-quadruplex structure from the human MYC promoter. *Nat. Chem. Biol.* **1**, 167–173 (2005).
30. Clancy, J.L. *et al.* mRNA isoform diversity can obscure detection of miRNA-mediated control of translation. *RNA* **17**, 1025–1031 (2011).
31. Green, J.J., Ying, L., Klenerman, D. & Balasubramanian, S. Kinetics of unfolding the human telomeric DNA quadruplex using a PNA trap. *J. Am. Chem. Soc.* **125**, 3763–3767 (2003).
32. Karttunen, J., Sanderson, S. & Shastri, N. Detection of rare antigen-presenting cells by the lacZ T-cell activation assay suggests an expression cloning strategy for T-cell antigens. *Proc. Natl. Acad. Sci. USA* **89**, 6020–6024 (1992).
33. Rodriguez, R. *et al.* A novel small molecule that alters shelterin integrity and triggers a DNA-damage response at telomeres. *J. Am. Chem. Soc.* **130**, 15758–15759 (2008).
34. Bugaut, A., Rodriguez, R., Kumari, S., Hsu, S.T. & Balasubramanian, S. Small molecule–mediated inhibition of translation by targeting a native RNA G-quadruplex. *Org. Biomol. Chem.* **8**, 2771–2776 (2010).
35. Huppert, J.L., Bugaut, A., Kumari, S. & Balasubramanian, S. G-quadruplexes: the beginning and end of UTRs. *Nucleic Acids Res.* **36**, 6260–6268 (2008).
36. Endoh, T., Kawasaki, Y. & Sugimoto, N. Suppression of gene expression by G-quadruplexes in open reading frames depends on G-quadruplex stability. *Angew. Chem. Int. Ed. Engl.* **52**, 5522–5526 (2013).
37. Apcher, S. *et al.* mRNA translation regulation by the Gly-Ala repeat of Epstein-Barr virus nuclear antigen 1. *J. Virol.* **83**, 1289–1298 (2009).
38. Khan, S. *et al.* Cutting edge: neosynthesis is required for the presentation of a T cell epitope from a long-lived viral protein. *J. Immunol.* **167**, 4801–4804 (2001).
39. Ostankovitch, M., Robila, V. & Engelhard, V.H. Regulated folding of tyrosinase in the endoplasmic reticulum demonstrates that misfolded full-length proteins are efficient substrates for class I processing and presentation. *J. Immunol.* **174**, 2544–2551 (2005).
40. Princiotta, M.F. *et al.* Quantitating protein synthesis, degradation, and endogenous antigen processing. *Immunity* **18**, 343–354 (2003).
41. Probst, H.C. *et al.* Immunodominance of an antiviral cytotoxic T cell response is shaped by the kinetics of viral protein expression. *J. Immunol.* **171**, 5415–5422 (2003).
42. Yewdell, J.W., Anton, L.C. & Bennink, J.R. Defective ribosomal products (DRiPs): a major source of antigenic peptides for MHC class I molecules? *J. Immunol.* **157**, 1823–1826 (1996).
43. Yewdell, J.W. & Haeryfar, S.M. Understanding presentation of viral antigens to CD8$^+$ T cells *in vivo*: the key to rational vaccine design. *Annu. Rev. Immunol.* **23**, 651–682 (2005).
44. Yewdell, J.W. & Nicchitta, C.V. The DRiP hypothesis decennial: support, controversy, refinement and extension. *Trends Immunol.* **27**, 368–373 (2006).
45. Li, L.C. *et al.* Small dsRNAs induce transcriptional activation in human cells. *Proc. Natl. Acad. Sci. USA* **103**, 17337–17342 (2006).
46. Norseen, J., Johnson, F.B. & Lieberman, P.M. Role for G-quadruplex RNA binding by Epstein-Barr virus nuclear antigen 1 in DNA replication and metaphase chromosome attachment. *J. Virol.* **83**, 10336–10346 (2009).
47. Bugaut, A. & Balasubramanian, S. 5′-UTR RNA G-quadruplexes: translation regulation and targeting. *Nucleic Acids Res.* **40**, 4727–4741 (2012).

Acknowledgments

We thank J. Shine and R. Tellam for valuable discussions, D. Hoang-Le and G. Wei for technical assistance and M. Di Antonio for providing PDS. Project grants (496684 and APP1005091) from the National Health and Medical Research Council (NHMRC) of Australia supported this research. J.T. was supported with a NHMRC Career Development Award Fellowship (no. 496712). R.K. is supported with a NHMRC Senior Principal Research Fellowship (APP1002476). The Balasubramanian group is supported by a program grant funded by Cancer Research UK.

Author contributions

P.M. designed and undertook the biophysical experiments and computational analyses and analyzed the data; J.T. and L.L. designed and generated the constructs; J.Z. performed the antigen presentation studies; N.P.C. and J.T. performed the SAXS experiments; J.L.C., J.T. and T.P. performed and analyzed the polysome experiments; S.B. and R.K. provided technical and scientific advice and comments on the manuscript. J.T. conceived the project, undertook the biochemical and immunological experiments and analyzed the data. J.T. and P.M. wrote the manuscript.

Competing financial interests

The authors declare no competing financial interests.

Additional information

Supplementary information is available in the online version of the paper. Reprints and permissions information is available online at http://www.nature.com/reprints/index.html. Correspondence and requests for materials should be addressed to J.T.

ONLINE METHODS

Cell lines. HEK293, EBNA1-expressing HEK293 (HEK293E) and H-2K^b–expressing HEK293 (HEK293KbC2) were cultured in Dulbecco modified Eagle medium supplemented with 10% FBS, 2 mM Glutamax and 100 IU/ml penicillin-streptomycin (DMEM growth medium). For the HEK293E cells, the DMEM growth medium was also supplemented with G418 (150 µg/mL). The B cell line (DG75) and a naturally infected lymphoblastoid cell line carrying an EBNA1 sequence from a B95-8 EBV BAC were maintained in RPMI 1640 supplemented with 2 mM L-glutamine, 100 IU/ml penicillin and 100 µg/ml streptomycin plus 10% FCS[15]. The LCL/EBV BAC culture medium was supplemented with puromycin (Sigma-Aldrich, St. Louis, Mo., USA) (1 µg/ml). The SIINFEKL-specific CD8$^+$ T-cell hybridoma (B3Z) was maintained in RPMI 1640 supplemented with 2 mM L-glutamine (Gibco, Life Technology), 1 mM sodium pyruvate (Gibco, Life Technology), 50 µM 2-mercaptoethanol (Gibco, Life Technology), 100 IU/ml penicillin and 100 µg/ml streptomycin plus 10% FCS (R-10).

Materials. Oligonucleotides were purchased from IBA GmbH or Sigma-Aldrich. The small molecule PDS was synthesized as previously described[33].

UV spectroscopy. UV melting curves were collected using a Varian Cary 400 Scan UV-visible spectrophotometer by following the absorbance at 295 nm. Oligonucleotides solutions were prepared at final concentrations of 2 µM, 4 µM, 8 µM or 16 µM in 10 mM lithium cacodylate (pH 7.2) containing 1 mM EDTA and 100 mM KCl. The samples were annealed by heating to 95 °C for 10 min and then slowly cooled to room temperature. Each sample was transferred to a quartz cuvette with 1-cm path length, covered with a layer of mineral oil, placed in the spectrophotometer and equilibrated at 5 °C for 10 min. Samples were then heated to 95 °C and cooled to 5 °C at a rate of 1 °C/min, with data collection every 1 °C during both melting and cooling. Melting temperature (T_m) values were obtained from the minimum of the first derivative of the melting curve. Thermal differential spectra were obtained by subtracting the spectra collected at 80 °C from the one collected at 25 °C for the oligonucleotide solutions as described above.

CD spectroscopy. CD experiments were conducted on a Chirascan spectropolarimeter using a quartz cuvette with an optical path length of 1 mm. Oligonucleotide solutions were prepared at a final concentration of 10 µM in 10 mM lithium cacodylate (pH 7.2) containing 1 mM of EDTA and 100 mM of KCl if not specified otherwise. The samples were annealed by heating at 95 °C for 10 min and slowly cooled to 20 °C. Scans were performed over the range of 200–320 nm at 25 °C. Each trace was the result of the average of three scans taken with a step size of 1 nm, a time per point of 1 s and a bandwidth of 1 nm. A blank sample containing only buffer was treated in the same manner and subtracted from the collected data. The data were finally baseline corrected at 320 nm.

NMR spectroscopy. ^{1}H NMR spectra were recorded at 278 K, 298 K and 318 K using a 500-MHz Bruker Avance 500 TCI spectrometer equipped with a cryogenic TCI ATM probe. Water suppression was achieved using excitation sculpting. The oligonucleotides were annealed in 10 mM PBS (pH 7.0) supplemented with 100 mM KCl and 10% D_2O at a final concentration of 0.1 mM. The samples were annealed by heating at 95 °C for 10 min and slowly cooled to 20 °C.

SAXS. SAXS data was measured using a SAXSess (Anton Paar) laboratory SAXS instrument. 100-µl samples of E1-GArN (1.86 mg/ml) or E1-GArM (1.73 mg/ml) were measured in and blanked against RNAase-free water (Promega) with exposure times of 20 min each. The scattering curves were monitored during the long exposure time as a test for radiation damage, which was not found to be an issue in this case. The SAXS data were normalized for concentration and an indirect Fourier transform performed using the program Gnom[48]. The mean square radius of the cross-section (R^2_{cs}) of the RNA is descriptive of the degree of secondary structure or self-association. R^2_{cs} was measured in a Q range between 0.7 and 1.7 nm^{-1} (ref. 49).

Fluorescence kinetic experiments. *Fluorescence kinetics experiments.* Fluorescence experiments were conducted on a Varian Cary Eclipse spectropolarimeter using a quartz cuvette with an optical path length of 1 cm. A dual-labeled g4-EBNA1 oligonucleotide, referred to as Fl-g4-EBNA1, was used. The donor fluorophore was 6-carboxyfluorescein (FAM), and the acceptor fluorophore was 6-carboxytetramethylrhodamine (TAMRA). For each kinetics assay solution containing Fl-g4-EBNA1, Fl-g4-EBNA1–AS2 or Fl-g4-EBNA1–PDS were prepared in 10 mM PBS buffer, pH 7.0, supplemented with 100 mM KCl, and the samples were equilibrated at 4 °C overnight. Kinetic assays were performed at 25 °C. AS2 or PDS were mixed at time (t) = 0. Samples were excited at 494 nm, and the emission at 580 nm was measured every 0.5 s for 10 min or 60 min.

FRET melting experiments. FRET experiments were carried out on a Roche LightCycler 480 system with a 200-nM oligonucleotide concentration in a 70-mM potassium cacodylate buffer, pH 7.4. The dual-labeled oligonucleotide, Fl-g4-EBNA1, was annealed at a concentration of 400 nM by heating at 95 °C for 10 min followed by slow cooling to 25 °C. 96-well plates were prepared by addition of 50 µl of the annealed DNA solution to each well, followed by addition of 50 µl solution of PDS. Measurements were made in triplicate with an excitation wavelength of 483 nm and a detection wavelength of 533 nm.

Polysome profiling, RNA extraction and RT-qPCR of polysome fractions. HEK293 cells (4.2×10^6) seeded in 15-cm^2 plates were transfected with 2 µg of EBNA1/pcDNA3 expression constructs of wild-type EBNA1 (E1-WT) and EBNA1 minus the GAr (E1-GA) and EBNA1 constructs expressing 500 nucleotides of either native GAr sequence (E1-GArN) or codon-modified GAr sequence (E1-GArM). 17 h after transfection, cells were harvested as described in ref. 30. Briefly, cells were incubated with 0.1 mg/mL cycloheximide for 3 min at 37 °C and lysed in 5 mM $MgCl_2$, 150 mM KCl, 20 mM HEPES (pH 7.6), 2 mM DTT, complete protease inhibitor (Roche), 0.5 mM PMSF, 0.1 mg/mL cycloheximide and 100 U/mL RNAseOUT (Invitrogen). Cleared lysate was applied to a 17–50% linear sucrose gradient and then centrifuged for 2.25 h at 35,000 r.p.m. in a SW 41 Ti rotor (Beckman), and fractions were collected. RNA extractions were performed as described in ref. 30. Each gradient fraction was spiked with 100 ng of yeast total RNA, 1.2 mL of ethanol was added, and then the fractions were stored overnight at −80 °C. Glycogen was added, and fractions were centrifuged at 20,000g for 20 min. The pellet was vortexed in 1 mL of Trizol (Life Technologies) for 30 min, and RNA was purified. Total cellular RNA was prepared from unfractionated lysate using Trizol. Purity was assessed by spectrophotometry, and integrity was assessed on an agarose gel. RNA preparations were treated with Turbo DNase (Ambion). One microgram of gradient fraction RNA was reverse transcribed using random hexamers and Superscript III (Life Technologies). All RT-qPCR was performed on a Lightcycler 480 using a SYBR master mix (Roche) and melt curve analysis. EBNA1 construct RT-qPCR results from polysome gradients were normalized to the spike-in. Primers used in the study were EBNA1 (forward) 5′-GGCGGCAGTGGACCTCAAAGAA-3′ and EBNA1 (reverse) 5′- TTGCAGCCAATGCAACTTGGACG-3′. Spike-in, *Saccharomyces cerevisiae*, NM_00117857.1 (209–432) CMD1 (forward) 5′-TGGCTCTGATGTCTCGTCAA-3′; CMD1 (reverse) 5′-CAAAGCAGCG AATTGTTGAA-3′.

IVT assays. To generate the EBNA1 transcripts for the biophysical studies, EBNA1 (nucleotides 209–566)/pcDNA3 expression constructs encoding 300 nucleotides of native GAr sequence (E1-GArN) or codon-modified GAr sequence (E1-GArM) were linearized with XbaI, and 1 µg of template was transcribed with T7 RNA polymerase, using a RiboMax *in vitro* transcription system (Promega). For IVT assays, EBNA1/pcDNA3 expression constructs encoding 300 or 400 nucleotides of either the native GAr sequence (E1-GArN) or the codon-modified GAr sequence (E1-GArM) were transcribed and translated with T7 RNA polymerase using a coupled transcription/translation reticulocyte lysate system (Promega) supplemented with 10 µCi [^{35}S]L-methionine (PerkinElmer, Mass., USA). Lysates were subjected to SDS-PAGE and autoradiography, as described in ref. 15. IVT assays using E1-GArN were also performed in the presence or absence of a range of antisense, sense strand and control deoxyoligonucleotides (**Supplementary Table 2**) at molar ratios of 10:1 and 20:1 to the EBNA1 mRNA repeat. Similar IVT assays were also performed in the presence or absence of the G-quadruplex–interacting drug PDS between 1–10 equivalents. Band intensities following densitometric analysis were quantified using ImageJ64 software.

EBNA1 translation efficiency determined after [^{35}S]methionine pulse labeling. HEK293 cells (4×10^5) were transiently transfected with either GFP-E1-WT, GFP-E1-GA or GFP-EBNA1 vectors expressing 500 nucleotides of either native GAr sequence (GFP-E1-GArN) or codon-modified GAr

sequence (GFP-E1-GArM). At 24 h after transfection, cells were washed in phosphate-buffered saline and incubated at 37 °C for 45 min in Met/Cys-free RPMI1640 medium (labeling medium) preceding a 20-min pulse at 37 °C in labeling medium containing 150 μCi/ml of EasyTag EXPRESS [^{35}S] Protein Labeling Mix (PerkinElmer, Mass., USA). Following the pulse, cells were lysed in Tris-buffered saline, including 0.3% Triton X-100, 0.2% NP-40 and protease inhibitors and pre-cleared with protein A Sepharose (GE Healthcare Australia), and lysates were immunoprecipitated with an antibody to GFP (A-6455, Life Technologies, 1:500). Immunoprecipitated samples were subjected to SDS-PAGE and analyzed by autoradiography. Band intensities following densitometric analysis were quantified using ImageJ64 software.

EBNA1 expression following treatment with antisense deoxyoligonucleotides. To assess EBNA1 expression *in vivo*, HEK293E cells (3.5×10^5) were transiently transfected with either a 21-mer antisense deoxyoligonucleotide (dAS2), a 20-mer sense strand deoxyoligonucleotide (dSS1) or a random 20-mer deoxyoligonucleotide, each at a final concentration of 200 nM, using Oligofectamine reagent (Invitrogen, Australia) according to the manufacturer's instructions. At 48 h after transfection, cells were washed and harvested, sonicated in Laemmli sample dye (Bio-Rad, Ca., USA) with 100 mM DTT and subjected to SDS-PAGE for immunoblotting with either a rabbit polyclonal antibody to EBNA1 (1:500) or a monoclonal antibody to β-actin (Clone AC-15, A5441, Sigma-Aldrich, 1:1,000) as described in ref. 14. The rabbit polyclonal antibody to EBNA1 was raised using a recombinant E1-ΔGAr protein. In addition, a naturally infected lymphoblastoid cell line carrying an EBNA1 sequence from a B95-8 EBV BAC[15] (D9wt LCL cells; 5×10^6) were transfected with 10 μg of either dAS2, dSS1 or a random deoxyolignucleotide by electroporation using a Bio-Rad Gene Pulser (960 μF, 250 V, 0.4-cm gap electrode, 300-μl assay volume, 25 °C) and incubated at 37 °C for 48 h. Cells were washed, sonicated in Laemmli sample buffer with 100 mM DTT and subjected to SDS-PAGE for immunoblotting with antibodies to EBNA1 or β-actin as described above. Band intensities following densitometric analysis were quantified using ImageJ64 software.

EBNA1 antigen presentation following treatment with antisense deoxyoligonucleotides. To assess EBNA1 endogenous processing, HEK293KbC2 cells (3.5×10^5) were seeded in DMEM growth medium without antibiotics so that they were 80% confluent at the time of transfection. The HEK293KbC2 cells were transfected together with 0.5 μg of an EBNA1-GFP expression vector encoding 400 nucleotides of native GAr sequence and expressing a sequence encoding a previously defined H-2K^b–restricted epitope SIINFEKL (referred to as SIIN), E1-GArN-SIIN-GFP[15] and 2.5 μg of either dAS2 or a control GAr sense strand deoxyoligonucleotide, dSS1 in a final volume of 2 ml using Lipofectamine 2000 Reagent (Invitrogen, Australia). To assess immune responses, the transfected target cells were harvested 48 h after transfection and incubated with a SIINFEKL-specific T-cell hybridoma (B3Z cells)[32] at 1:1, 1:0.5, 1:0.25 or 1:0.125 effector/target cell ratios for 18 h. B3Z cells were harvested and stained as described below under B3Z T-cell activation assay method.

EBNA1 expression in the presence of the G-quadruplex ligand (PDS). For EBNA1 *in vivo* expression experiments, HEK293 cells (3.5×10^5) were pretreated with PDS at a final concentration of 2 μM, 4 μM or 8 μM for 45 min. The cells were then transiently transfected with 0.4 μg of an EBNA1-GFP expression construct encoding 400 nucleotides of native GAr sequence, E1-GArN-GFP, using Effectene (QIAGEN, Hilden, Germany) according to the manufacturer's instructions. DG75 cells (2×10^6) were transiently transfected with 2 μg of E1-GArN-GFP using the Amaxa Cell Line Nucleofector Kit V (Lonza, Cologne, Germany) in the presence or absence of PDS at a final concentration of 2 μM, 4 μM or 8 μM. At 24 h after transfection, cells were harvested and analyzed for GFP expression by flow cytometry on a FACSCanto (BD Biosciences).

EBNA1 antigen presentation in the presence of the G-quadruplex ligand (PDS). For the assessment of EBNA1 endogenous processing, HEK293KbC2 cells (3.5×10^5) were transiently transfected with 0.4 μg E1-GArN-SIIN-GFP in the presence or absence of PDS at a final concentration of 2 μM, 4 μM or 8 μM. Cells were harvested and sorted for GFP-positive cells on a FACSAria cell sorter (BD Biosciences) 24 h after transfection and incubated with SIINFEKL-specific T-cell hybridoma (B3Z cells) at a 1:1 E/T ratio for 18 h. B3Z cells were harvested and stained as described below under the B3Z T-cell activation assay method.

B3Z T-cell activation assay. B3Z is a T-cell hybridoma expressing a TCR that is specifically activated by the Ovalbumin (257–264) peptide, (SIINFEKL) in the context of H-2Kb. The cells express the LacZ gene under the control of the nuclear factor of activated T-cell (NF-AT) element of the interleukin 2 enhancer, thereby allowing the activation of B3Z T cells to be measured by β-galactosidase activity in single cells[32]. Following incubation of the SIINFEKL-expressing EBNA1 transfectants with B3Z cells at the stated effector/target cell ratios for 18 h, B3Z cells were harvested and stained with APC-anti-mouse CD3e (Clone 145-2C11, 553066, BD Pharmingen, 1:66) and PE-anti-mouse CD8 antibodies (Clone 53-6.7, 553033, BD Pharmingen, 1:100), followed by osmotic loading of FDG (fluorescein di-β-galactoside; Invitrogen), as previously described[50]. Briefly, B3Z cells were resuspended in 25 μl staining buffer (PBS containing 4% FBS and 10 mM HEPES, pH 7.2) and incubated for 10 min at 37 °C, followed by the addition of 25 μl prewarmed FDG (2 mM in de-ionized water). After a further incubation at 37 °C for 1 min, 450 μl ice-cold staining buffer containing 1 μg/ml 7-aminoactino-mycin D (7-AAD) was added to each sample to stop osmotic loading. The activation of B3Z T-cells (gated on 7-AAD$^-$ CD3$^+$ CD8$^+$ cells) was assessed using flow cytometry on a FACSCanto (BD Biosciences) to measure the fluorescein di-β-galactoside (FDG) as an indicator of intracellular β-galactosidase activity.

Statistical analysis. For the statistical analysis of the IVT and antigen presentation experiments, a two-tailed paired Student's *t*-test was used.

48. Svergun, D.I. Determination of the regularization parameter in indirect-transform methods using perceptual criteria. *J. Appl. Crystallogr.* **25**, 495–503 (1992).
49. Porod, G. in *Small Angle X-ray Scattering* (eds. Glatter, O. & Kratky, O.) 17–51 (Academic Press, London, 1982).
50. Nolan, G.P., Fiering, S., Nicolas, J.F. & Herzenberg, L.A. Fluorescence-activated cell analysis and sorting of viable mammalian cells based on β-D-galactosidase activity after transduction of *Escherichia coli* lacZ. *Proc. Natl. Acad. Sci. USA* **85**, 2603–2607 (1988).

doi:10.1038/nchembio.1479

ERRATA

G quadruplexes regulate Epstein-Barr virus–encoded nuclear antigen 1 mRNA translation

Pierre Murat, Jie Zhong, Lea Lekieffre, Nathan P Cowieson, Jennifer L Clancy, Thomas Preiss, Shankar Balasubramanian, Rajiv Khanna & Judy Tellam

Nat. Chem. Biol.; doi:10.1038/nchembio.1479; corrected online 4 April 2014

In the version of this article initially published online, the third subheading in the Results subsection was incorrectly written as "Destabilizing G-quadruplexes mRNA translation"; it should read "Destabilizing G-quadruplexes enhances mRNA translation". Also, 'Cambridge Research Institute', as listed under the Affiliations, should be 'Cambridge Institute', and the last line of the Acknowledgments, originally written as "P.M. is supported by Cancer Research UK.", should read "The Balasubramanian group is supported by a program grant funded by Cancer Research UK." These errors have been corrected for the print, PDF and HTML versions of this article.